Linear optical properties in the projector-augmented wave methodology

M. Gajdoš, K. Hummer, and G. Kresse*
Institut für Materialphysik and Center for Computational Materials Science, Universität Wien, Sensengasse 8/12, A-1090 Wien, Austria

J. Furthmüller and F. Bechstedt
Institut für Festkörpertheorie and Theoretische Optik, Friedrich-Schiller-Universität, D-07743 Jena, Germany
(Received 13 September 2005; published 17 January 2006)

In this work we derive closed expressions for the head of the frequency-dependent microscopic polarizability matrix in the projector-augmented wave (PAW) methodology. Contrary to previous applications, the longitudinal expression is utilized, resulting in dielectric properties that are largely independent of the applied potentials. The improved accuracy of the present approach is demonstrated by comparing the longitudinal and transversal expressions of the polarizability matrix for a number of cubic semiconductors and one insulator, i.e., Si, SiC, AlP, GaAs, and diamond (C), respectively. The methodology is readily extendable to more complicated nonlocal Hamiltonians or to the calculation of the macroscopic dielectric matrix including local field effects in the random phase or density functional approximation, which is demonstrated for the previously mentioned model systems. Furthermore, density functional perturbation theory is extended to the PAW method, and the respective results are compared to those obtained by summation over the conduction band states.

DOI: 10.1103/PhysRevB.73.045112 PACS number(s): 31.15.Md, 78.20.Bh, 78.20.Ci

I. INTRODUCTION

The evaluation of the static and frequency-dependent dielectric response functions, such as absorption, reflectance, or energy loss spectra, is important for the interpretation of the optical properties measured for bulk semiconductors and metals as well as their surfaces. Although it is now generally accepted that an accurate quantitative description requires a treatment beyond the independent particle picture, a qualitative agreement between theory and experiment can often be achieved on the level of density functional theory (DFT), i.e., the Kohn-Sham eigenvalues and their eigenfunctions. Furthermore, the evaluation of the frequency-dependent polarizability matrices is crucial for the implementation of most post-DFT schemes, such as *GW*,[1] exact-exchange optimized-effective-potential methods,[2] or the Bethe-Salpeter equation,[3,4] which constitute the main routes toward a high-level description of the optical properties in extended systems.[5–7]

An efficient calculation of the frequency-dependent microscopic polarizability matrix χ is therefore important. Closed expressions for periodic systems have been derived by Adler[8] and Wiser[9] in connection with the self-consistent field approach. In this context, a crucial problem is the determination of the long-wavelength limit $\mathbf{q}\rightarrow\mathbf{0}$ of the frequency-dependent microscopic polarizability and dielectric matrices, which essentially determines the optical properties in the wavelength regime accessible to optical or electronic probes. The frequency-dependent macroscopic dielectric constants are also important for *GW* calculations, where they are required for analytically integrating the $\mathbf{q}=\mathbf{0}$ Coulomb singularity of the correlation and self-energy.[1] Dielectrically screened interaction potentials are also necessary, if excitonic effects are included in the description of optical properties.[10,11]

Since the polarizability matrix shows a nonanalytic behavior around $\mathbf{q}\rightarrow\mathbf{0}$, the straightforward extrapolation from a finite $\mathbf{q}$ is slowly converging. This difficulty is usually dealt with by performing a Taylor or $\mathbf{k}\cdot\mathbf{p}$ expansion of the wave functions for small momentum transfers.[1,12] For purely local potentials, this results in a fairly simple expression with the transition operator between two states being proportional to the momentum (or ∇) operator. This is the so-called transversal approximation, where *transversal* is related to the coupling of a field to electrons in the transversal gauge. Such an approach is usually applied in the context of full potential codes, which are employing large and complete basis sets and are considering the final ground-state wave functions to be essentially exact solutions to the local one-electron potential.

However, if nonlocal pseudopotentials $V(\mathbf{r},\mathbf{r}')$ or nonlocal exchange interactions $V_x(\mathbf{r},\mathbf{r}')$ are considered, the simple transversal approximation breaks down and an additional commutator involving the nonlocal potential and the position operator enters the formalism. Further complications arise, if the pseudo-wave-functions are not properly normalized, as is the case in the projector-augmented wave (PAW) method.[13] With few exceptions, the evaluation of optical properties within the longitudinal formalism has therefore been limited to norm-conserving pseudopotentials, for which the appropriate expressions have been derived almost two decades ago.[1,12] The major contribution of the present work is the extension of these ideas to the PAW method, i.e., the derivation of exact closed expressions for the long-wavelength limit of the polarizability matrix in the PAW method. Compared to standard norm-conserving pseudopotentials, the PAW method has one important advantage: it allows for a significant reduction of the plane wave cutoffs at the same high level of accuracy. Consequently, the application of this method to systems containing strongly localized *d* or *f* electrons is straightforward. Furthermore, the PAW method incorporates the exact nodal structure of the valence electron's wave functions.[13]

In order to derive the required expressions, we start from the original Adler and Wiser formulation[8,9] and perform a Taylor expansion of the wave functions for transitions with a small momentum transfer **q**. Because of the existence of an overlap operator, the evaluation of the long-wavelength limit in the longitudinal approximation involves dipole terms, which are absent in standard pseudopotential methods. For four model semiconductors, i.e., Si, SiC, AlP, and GaAs, and one insulator (diamond, C) the static and dynamic dielectric matrix are evaluated using the longitudinal formalism. Our findings are compared to the results obtained by the transversal approximation, which has been previously used in the context of the PAW methodology by Adolph, Furthmüller, and Bechstedt.[6] Both expressions yield almost exactly identical results in the limit of a complete PAW one-center basis set. However, this limit is in practice not always reached, and hence the present longitudinal expression should be preferred over the simpler transversal one. Furthermore, we briefly introduce closed formulas to calculate dielectric properties using density functional perturbation theory within the PAW framework.[14–16]

Section II introduces the theoretical framework. Therein the PAW methodology, the longitudinal and transversal expressions for the head of the dielectric matrix, and density functional perturbation theory are discussed. Technical details, such as the PAW data sets and k-point grids are summarized in Sec. III. Section IV presents results for the static and the dynamic dielectric matrix in the random phase and density functional approximation with and without inclusion of local field effects. The last section summarizes the main achievements of this work and the conclusions therefrom.

II. THEORY

A. Basics of the PAW formalism

In this subsection we will discuss the basic concepts of the PAW method, which are necessary to understand the evaluation of the response functions within this formalism (see Ref. 13; the notation follows Ref. 17).

In the PAW method, the one-electron wave functions $\psi_{n\mathbf{k}}$ are derived from the pseudo-wave-functions $\tilde{\psi}_{n\mathbf{k}}$ by means of a linear transformation:[13]

$$|\psi_{n\mathbf{k}}\rangle = |\tilde{\psi}_{n\mathbf{k}}\rangle + \sum_i (|\phi_i\rangle - |\tilde{\phi}_i\rangle)\langle\tilde{p}_i|\tilde{\psi}_{n\mathbf{k}}\rangle. \tag{1}$$

The pseudo-orbitals $\tilde{\psi}_{n\mathbf{k}}$, where n is the band index and $\mathbf{k}$ the Bloch wave vector, are the variational quantities which are expanded in the reciprocal space using plane waves. The index i is a shorthand for the atomic site $\mathbf{R}_i$, the angular momentum quantum numbers l_i, m_i, and an additional index ε_i referring to the reference energy. The all-electron (AE) partial waves ϕ_i are solutions of the radial Schrödinger equation for a non-spin-polarized reference atom at specific energies ε_i and for a specific angular momentum l_i. The pseudo-partial-waves $\tilde{\phi}_i$ are equivalent to the AE partial waves outside a core radius r_c and match continuously onto ϕ_i inside the core radius. The projector functions $\tilde{p}_i$ are dual to the partial waves:

$$\langle\tilde{p}_i|\tilde{\phi}_j\rangle = \delta_{ij}. \tag{2}$$

Furthermore, the projector functions $\tilde{p}_i$ depend on the distance from the center of the PAW sphere on which they are localized,

$$\langle\mathbf{r}|\tilde{p}_i\rangle = \tilde{p}_i(\mathbf{r} - \mathbf{R}_i), \tag{3}$$

where $\mathbf{R}_i$ is the position of the atom i.

Introducing the cell periodic part $|\tilde{u}_{n\mathbf{k}}\rangle$ of the pseudo-wave-function one can write

$$|\tilde{\psi}_{n\mathbf{k}}\rangle = e^{i\mathbf{k}\mathbf{r}}|\tilde{u}_{n\mathbf{k}}\rangle. \tag{4}$$

It is convenient to define $\mathbf{k}$-dependent projector functions $|\tilde{p}_{i\mathbf{k}}\rangle$ as well:

$$|\tilde{p}_{i\mathbf{k}}\rangle = e^{-i\mathbf{k}(\mathbf{r}-\mathbf{R}_i)}|\tilde{p}_i\rangle. \tag{5}$$

With this definition one can rewrite $\langle\tilde{p}_i|\tilde{\psi}_{n\mathbf{k}}\rangle$ as

$$\langle\tilde{p}_i|\tilde{\psi}_{n\mathbf{k}}\rangle = e^{i\mathbf{k}\mathbf{R}_i}\langle\tilde{p}_{i\mathbf{k}}|\tilde{u}_{n\mathbf{k}}\rangle. \tag{6}$$

In the frequently occurring terms involving[17]

$$\sum_{ij} \langle\tilde{\psi}_{n\mathbf{k}}|\tilde{p}_i\rangle D_{ij}\langle\tilde{p}_j|\tilde{\psi}_{n\mathbf{k}}\rangle = \sum_{ij} \langle\tilde{u}_{n\mathbf{k}}|\tilde{p}_i\rangle D_{ij}\langle\tilde{p}_j|\tilde{u}_{n\mathbf{k}}\rangle \tag{7}$$

the phase factor $e^{-i\mathbf{k}\mathbf{R}_j}e^{i\mathbf{k}\mathbf{R}_i}$ drops out, because the pair of indices i and j are restricted to a single sphere, i.e., $\mathbf{R}_i = \mathbf{R}_j$.

B. Polarizability and dielectric matrices

For a translationally invariant system, the Fourier transform of the frequency-dependent symmetric dielectric matrix in the random phase approximation[18] (RPA) is given by

$$\varepsilon_{\mathbf{G},\mathbf{G}'}(\mathbf{q},\omega) = \delta_{\mathbf{G},\mathbf{G}'} - \frac{4\pi e^2}{|\mathbf{G}+\mathbf{q}||\mathbf{G}'+\mathbf{q}|}\chi^0_{\mathbf{G},\mathbf{G}'}(\mathbf{q},\omega), \tag{8}$$

where $\mathbf{G}$ and $\mathbf{G}'$ are reciprocal lattice vectors and $\mathbf{q}$ stands for the Bloch vector of the incident wave. The matrix $\chi^0(\mathbf{q},\omega)$ is the irreducible polarizability matrix in the independent particle picture as derived by Adler and Wiser[8,9] in the context of the self-consistent field approach. In the Bloch notation it can be written as[12]

$$\chi^0_{\mathbf{G},\mathbf{G}'}(\mathbf{q},\omega) = \frac{1}{\Omega}\sum_{n,n',\mathbf{k}} 2w_{\mathbf{k}}(f_{n'\mathbf{k}+\mathbf{q}} - f_{n\mathbf{k}}) \times \frac{\langle\psi_{n'\mathbf{k}+\mathbf{q}}|e^{i(\mathbf{q}+\mathbf{G})\mathbf{r}}|\psi_{n\mathbf{k}}\rangle\langle\psi_{n\mathbf{k}}|e^{-i(\mathbf{q}+\mathbf{G}')\mathbf{r}'}|\psi_{n'\mathbf{k}+\mathbf{q}}\rangle}{\epsilon_{n'\mathbf{k}+\mathbf{q}} - \epsilon_{n\mathbf{k}} - \omega - i\eta}, \tag{9}$$

where η is an infinitesimal number and Ω the volume of the primitive cell. While the k-point weights $w_{\mathbf{k}}$ are defined such that they sum to 1, the Fermi weights f equal 1 for occupied and zero for unoccupied states. The factor 2 before the weights accounts for the fact that we consider a spin-degenerate system.

Mind that the frequency ω has the dimension of an energy, and that we have adopted the commonly used notation

$$\langle \psi_{n'\mathbf{k}+\mathbf{q}} | e^{i(\mathbf{q}+\mathbf{G})\mathbf{r}} | \psi_{n\mathbf{k}} \rangle \equiv \int_\Omega e^{i(\mathbf{q}+\mathbf{G})\mathbf{r}} \psi^*_{n'\mathbf{k}+\mathbf{q}}(\mathbf{r}) \psi_{n\mathbf{k}}(\mathbf{r}) d^3\mathbf{r}$$
$$= \langle u_{n'\mathbf{k}+\mathbf{q}} | e^{i\mathbf{G}\mathbf{r}} | u_{n\mathbf{k}} \rangle$$
$$\equiv \int_\Omega e^{i\mathbf{G}\mathbf{r}} u^*_{n'\mathbf{k}+\mathbf{q}}(\mathbf{r}) u_{n\mathbf{k}}(\mathbf{r}) d^3\mathbf{r}. \quad (10)$$

The evaluation of the macroscopic dielectric matrix $\varepsilon_\infty(\mathbf{q},\omega)$ requires an inversion of the full microscopic dielectric matrix and taking the limit $\mathbf{q}\to\mathbf{0}$:

$$\frac{1}{\varepsilon_\infty(\hat{\mathbf{q}},\omega)} = \lim_{\mathbf{q}\to 0} \varepsilon^{-1}_{0,0}(\mathbf{q},\omega). \quad (11)$$

Here the local field effects are included in the Hartree approximation (or RPA). The dielectric function depends on the direction $\hat{\mathbf{q}}=\mathbf{q}/|\mathbf{q}|$, which is used to approach the Γ point (see below). If the off-diagonal elements of the dielectric matrix (local field effects) are neglected, the macroscopic dielectric function can be approximated by the head of the microscopic dielectric matrix:

$$\varepsilon_\infty(\hat{\mathbf{q}},\omega) \approx \lim_{\mathbf{q}\to 0} \varepsilon_{0,0}(\mathbf{q},\omega). \quad (12)$$

In this simplification the imaginary part of the macroscopic dielectric function $\varepsilon^{(2)}_\infty(\hat{\mathbf{q}},\omega)$ is given by

$$\varepsilon^{(2)}_\infty(\hat{\mathbf{q}},\omega) = \frac{4\pi^2 e^2}{\Omega} \lim_{\mathbf{q}\to 0} \frac{1}{|\mathbf{q}|^2} \sum_{c,v,\mathbf{k}} 2w_\mathbf{k} \delta(\epsilon_{c\mathbf{k}+\mathbf{q}} - \epsilon_{v\mathbf{k}} - \omega)$$
$$\times |\langle u_{c\mathbf{k}+\mathbf{q}} | u_{v\mathbf{k}} \rangle|^2, \quad (13)$$

where the indices c and v are restricted to the conduction and the valence band states, respectively. The dielectric function depends on the direction $\hat{\mathbf{q}}$ via the equation

$$\varepsilon_\infty(\hat{\mathbf{q}},\omega) = \lim_{\mathbf{q}\to 0} \varepsilon_\infty(\mathbf{q},\omega) = \sum_{\alpha,\beta} \hat{\mathbf{q}}_\alpha \varepsilon_{\alpha\beta}(\omega) \hat{\mathbf{q}}_\beta. \quad (14)$$

Here $\hat{\mathbf{q}}_\alpha$ is one Cartesian component of the unit vector $\hat{\mathbf{q}}$, and the 3×3 Cartesian tensor $\varepsilon_{\alpha\beta}$ is defined as

$$\varepsilon^{(2)}_{\alpha\beta}(\omega) = \frac{4\pi^2 e^2}{\Omega} \lim_{q\to 0} \frac{1}{q^2} \sum_{c,v,\mathbf{k}} 2w_\mathbf{k} \delta(\epsilon_{c\mathbf{k}} - \epsilon_{v\mathbf{k}} - \omega)$$
$$\times \langle u_{c\mathbf{k}+\mathbf{e}_\alpha q} | u_{v\mathbf{k}} \rangle \langle u_{c\mathbf{k}+\mathbf{e}_\beta q} | u_{v\mathbf{k}} \rangle^*. \quad (15)$$

The vectors $\mathbf{e}_\alpha$ are unit vectors for the three Cartesian directions. In the calculation of $\varepsilon^{(2)}_{\alpha\beta}$, it is possible to restrict $\mathbf{k}$ to the irreducible wedge of the Brillouin zone of the crystal symmetry group, if the final matrix is symmetrized applying the symmetry group of the crystal. The real part of the dielectric tensor $\varepsilon^{(1)}_{\alpha\beta}$ is finally obtained by the usual Kramers-Kronig transformation

$$\varepsilon^{(1)}_{\alpha\beta}(\omega) = 1 + \frac{2}{\pi} \mathrm{P} \int_0^\infty \frac{\varepsilon^{(2)}_{\alpha\beta}(\omega')\omega'}{\omega'^2 - \omega^2} d\omega', \quad (16)$$

where P denotes the principal value.

The difficulty in this approach is the required evaluation of the first-order change of the wave function $\psi_{c\mathbf{k}+\mathbf{q}}$ with respect to $\mathbf{q}$. Although not particularly time consuming, the implementation is rather involved for most electronic structure methods.

Particularly in full-potential codes,[19] it is therefore common to determine the imaginary part of the dielectric function using the simpler transversal expression

$$\varepsilon^{(2)}_{\alpha\beta}(\omega) = \frac{4\pi^2 e^2 \hbar^4}{\Omega \omega^2 m_e^2} \lim_{\mathbf{q}\to\mathbf{0}} \sum_{c,v,\mathbf{k}} 2w_\mathbf{k} \delta(\epsilon_{c\mathbf{k}+\mathbf{q}} - \epsilon_{v\mathbf{k}} - \omega)$$
$$\times \langle u_{c\mathbf{k}} | i\nabla_\alpha - \mathbf{k}_\alpha | u_{v\mathbf{k}} \rangle \langle u_{c\mathbf{k}} | i\nabla_\beta - \mathbf{k}_\beta | u_{v\mathbf{k}} \rangle^*. \quad (17)$$

This expression is readily obtained from Eq. (13) using second-order perturbation theory in $\mathbf{k}$ and the relationship[1,12]

$$\frac{\partial \mathbf{H}(\mathbf{k})}{\partial \mathbf{k}} = i[\mathbf{H}(\mathbf{k}), \mathbf{r}] = -i\frac{\hbar^2}{m_e}(\nabla + i\mathbf{k}), \quad (18)$$

where $\mathbf{H}(\mathbf{k})$ is the effective one-electron Hamiltonian for the cell periodic wave functions at the k-point $\mathbf{k}$:

$$\mathbf{H}(\mathbf{k}) = -\frac{\hbar^2}{2m_e}(\nabla + i\mathbf{k})^2 + V. \quad (19)$$

It is, however, important to realize that Eq. (18) holds for a purely local one-electron potential $V(\mathbf{r})$ only. For nonlocal pseudopotentials the potential operator is—as the name already suggests—nonlocal, and concomitantly the commutator of the Hamiltonian and the position operator differs from the nabla operator.[20] Therefore the longitudinal or appropriate corrections to the transversal expression have to be used, when pseudopotentials are applied.[1,12,21] As we will see below the same holds at least in principle for the PAW method. If Eq. (18) is directly applied to the PAW method neglecting these nonlocal terms, a plane wave part and a one-center correction are obtained:[6]

$$\langle u_{c\mathbf{k}} | i\,\nabla - \mathbf{k} | u_{v\mathbf{k}} \rangle = \langle \tilde{u}_{c\mathbf{k}} | i\,\nabla - \mathbf{k} | \tilde{u}_{v\mathbf{k}} \rangle + \sum_{ij} \langle \tilde{u}_{c\mathbf{k}} | \tilde{p}_{i\mathbf{k}} \rangle \langle \tilde{p}_{j\mathbf{k}} | \tilde{u}_{v\mathbf{k}} \rangle$$
$$\times i[\phi_i(\mathbf{r})\,\nabla\,\phi_j(\mathbf{r}) - \tilde{\phi}_i(\mathbf{r})\,\nabla\,\tilde{\phi}_j(\mathbf{r})]. \quad (20)$$

In the following, a closed expression for the head of the dielectric matrix in the alternative longitudinal form is derived within the PAW framework taking the nonlocality of the Hamilton operator fully into account.

Before continuing with the derivation of the longitudinal form of the dielectric matrix, we want to point out the important difference between the PAW and the full-potential linearized augmented plane wave (FLAPW) method which necessitates the application of the longitudinal expression in the former. Compared to the latter, the one-center terms in the PAW method are truncated at rather low angular momenta. As a consequence, the transversal expression becomes inaccurate, in particular for standard PAW potentials, which usually truncate the one-center expansion at $l=1$ for $2p$ and $3p$ elements.[13] In principle, this problem can be remedied by including higher angular components in the one-center terms.[6] However, the rigorous treatment using the exact longitudinal form has the advantage of a more rapid convergence with the one-center basis set. Furthermore, the extension of the longitudinal expression to nonlocal ex-

change correlation functionals, e.g., functionals that include the exact Hartree-Fock exchange, is readily achievable.[21–23]

C. Charge density kernel for Bloch wave functions in the PAW method

For the evaluation of Eq. (9) in the PAW formalism, the crucial quantity is the cell periodic part of the density matrix

$$B_{n'\mathbf{k}+\mathbf{q},n\mathbf{k}}(\mathbf{r}) \equiv e^{i\mathbf{q}\mathbf{r}}\psi^*_{n'\mathbf{k}+\mathbf{q}}(\mathbf{r})\psi_{n\mathbf{k}}(\mathbf{r}), \tag{21}$$

which needs to be Fourier transformed in order to calculate the polarizability [Eq. (10)]. To evaluate the body ($\mathbf{G}+\mathbf{q} \neq 0$) of the dielectric matrix we use the mixed space approach suggested in Refs. 24 and 25. Using the relation between the pseudo-wave-function $\tilde{\psi}$ and the AE wave function ψ [Eq. (1)] together with the usual completeness relation[13] and introduction of the cell periodic wave functions and projectors [Eqs. (4) and (6)] yield

$$B_{n'\mathbf{k}+\mathbf{q},n\mathbf{k}}(\mathbf{r}) = \tilde{u}^*_{\mathbf{n}'\mathbf{k}+\mathbf{q}}(\mathbf{r})\tilde{u}_{n\mathbf{k}}(\mathbf{r}) + \sum_{ij} \langle \tilde{u}_{n'\mathbf{k}+\mathbf{q}}|\tilde{p}_{i\mathbf{k}+\mathbf{q}}\rangle\langle\tilde{p}_{j\mathbf{k}}|\tilde{u}_{n\mathbf{k}}\rangle \times e^{i\mathbf{q}(\mathbf{r}-\mathbf{R}_i)}[\phi_i(\mathbf{r})\phi_j(\mathbf{r}) - \tilde{\phi}_i(\mathbf{r})\tilde{\phi}_j(\mathbf{r})]. \tag{22}$$

We represent the augmentation charges on the plane wave grid only and neglect one-center terms. The quantity $\tilde{u}^*_{n'\mathbf{k}+\mathbf{q}}(\mathbf{r})\tilde{u}_{n\mathbf{k}}(\mathbf{r})$ is evaluated in real space and proper augmentation charges are also added in real space to account for the fact that the wave functions are not normalized in the PAW method:

$$B_{n'\mathbf{k}+\mathbf{q},n\mathbf{k}}(\mathbf{r}) \approx \tilde{u}^*_{n'\mathbf{k}+\mathbf{q}}(\mathbf{r})\tilde{u}_{n\mathbf{k}}(\mathbf{r}) + \sum_{ij,LM} \langle \tilde{u}_{n'\mathbf{k}+\mathbf{q}}|\tilde{p}_{i\mathbf{k}+\mathbf{q}}\rangle\langle\tilde{p}_{j\mathbf{k}}|\tilde{u}_{n\mathbf{k}}\rangle \times e^{i\mathbf{q}(\mathbf{r}-\mathbf{R}_i)}\hat{Q}^{LM}_{ij}(\mathbf{r}). \tag{23}$$

For details we refer to the implementation of the exact exchange operator discussed in Secs. II B and II D 1 of Ref. 22. The final charge density $B_{n'\mathbf{k}+\mathbf{q},n\mathbf{k}}(\mathbf{r})$ is fast Fourier transformed to reciprocal space and then added to the polarizability matrix [Eqs. (9) and (10)]. After the Fourier transformation, additionally, the same cutoff is imposed on the resultant charge density as on the wave functions. The size of the basis set for the polarizability matrix is therefore identical to the basis set of the wave functions at the point $\mathbf{q}$.

As already emphasized, we neglect the one-center (onsite) PAW terms in Eq. (22), i.e., only the plane wave contributions are taken into account. This approximation is expected to be accurate, since the difference between the pseudo- and AE wave functions is only in the short-wavelength range and the respective local field contributions are small, because they are weighted by $1/|\mathbf{G}||\mathbf{G}'|$ [Eq. (8)].

D. Long-wavelength limit in the PAW method

The head and the wings of the polarizability ($\mathbf{G}+\mathbf{q}\rightarrow\mathbf{0}$) are more difficult to evaluate. They are calculated by expanding the wave functions linearly around each k point and evaluating the derivative of the pseudo-wave-functions with respect to $\mathbf{q}$ as suggested in Refs. 1 and 12.

To determine $\lim_{\mathbf{q}\rightarrow\mathbf{0}}\langle\psi_{n'\mathbf{k}+\mathbf{q}}|e^{i\mathbf{q}\mathbf{r}}|\psi_{n\mathbf{k}}\rangle$, the exponential is expanded to first order around $\mathbf{q}=\mathbf{0}$ in Eq. (22),

$$e^{i\mathbf{q}(\mathbf{r}-\mathbf{R}_i)} = 1 + i\mathbf{q}(\mathbf{r}-\mathbf{R}_i) + o(\mathbf{q}^2), \tag{24}$$

resulting in

$$\lim_{\mathbf{q}\rightarrow\mathbf{0}}\langle\psi_{n'\mathbf{k}+\mathbf{q}}|e^{i\mathbf{q}\mathbf{r}}|\psi_{n\mathbf{k}}\rangle = \int_\Omega B_{n'\mathbf{k}+\mathbf{q},n\mathbf{k}}(\mathbf{r})d^3\mathbf{r} = \langle\tilde{u}_{n'\mathbf{k}+\mathbf{q}}|\left(1+\sum_{ij}|\tilde{p}_{i\mathbf{k}+\mathbf{q}}\rangle Q_{ij}\langle\tilde{p}_{j\mathbf{k}}|\right)|\tilde{u}_{n\mathbf{k}}\rangle + i\mathbf{q}\sum_{ij}\langle\tilde{u}_{n'\mathbf{k}+\mathbf{q}}|\tilde{p}_{i\mathbf{k}+\mathbf{q}}\rangle\vec{\tau}_{ij}\langle\tilde{p}_{j\mathbf{k}}|\tilde{u}_{n\mathbf{k}}\rangle, \tag{25}$$

where Q_{ij} and $\vec{\tau}_{ij}$ are the norm and the dipole moments of the one-center charge densities:

$$Q_{ij} = \int_{\Omega_{\mathrm{PAW}}}[\phi_i(\mathbf{r})\phi_j(\mathbf{r}) - \tilde{\phi}_i(\mathbf{r})\tilde{\phi}_j(\mathbf{r})]d^3\mathbf{r},$$

$$\vec{\tau}_{ij} = \int_{\Omega_{\mathrm{PAW}}}(\mathbf{r}-\mathbf{R}_i)[\phi_i(\mathbf{r})\phi_j(\mathbf{r}) - \tilde{\phi}_i(\mathbf{r})\tilde{\phi}_j(\mathbf{r})]d^3\mathbf{r}. \tag{26}$$

To emphasize that $\vec{\tau}_{ij}$ is a vector quantity with three Cartesian components, we explicitly use the vector notation here. It is important to realize that $\vec{\tau}_{ij}$ is well defined, because the centers of the PAW spheres $\mathbf{R}_i$ are subtracted.

In the final step, the cell periodic part of the wave function $\tilde{u}_{n\mathbf{k}+\mathbf{q}}$ is replaced by the Taylor expansion around $\tilde{u}_{n\mathbf{k}}$, where the quadratic terms are neglected:

$$\tilde{u}_{n\mathbf{k}+\mathbf{q}} = \tilde{u}_{n\mathbf{k}} + \mathbf{q}\boldsymbol{\nabla}_{\mathbf{k}}\tilde{u}_{n\mathbf{k}} + o(\mathbf{q}^2). \tag{27}$$

Furthermore, the changes of the projectors with respect to $\mathbf{k}$ are required to linear order [cf. Eq. (5)]:

$$|\tilde{p}_{i\mathbf{k}+\mathbf{q}}\rangle = [1 - i\mathbf{q}(\mathbf{r}-\mathbf{R}_i)]|\tilde{p}_{i\mathbf{k}}\rangle + o(\mathbf{q}^2). \tag{28}$$

After some straightforward manipulation the following relationship is obtained:

$$\lim_{\mathbf{q}\rightarrow\mathbf{0}}\langle\psi_{n'\mathbf{k}+\mathbf{q}}|e^{i\mathbf{q}\mathbf{r}}|\psi_{n\mathbf{k}}\rangle = \langle\tilde{u}_{n'\mathbf{k}}|\left(1+\sum_{ij}|\tilde{p}_{i\mathbf{k}}\rangle Q_{ij}\langle\tilde{p}_{j\mathbf{k}}|\right)|\tilde{u}_{n\mathbf{k}}\rangle + |\mathbf{q}|\langle\hat{\mathbf{q}}\vec{\beta}_{n'\mathbf{k}}|\tilde{u}_{n\mathbf{k}}\rangle, \tag{29}$$

where $\hat{\mathbf{q}}=\mathbf{q}/|\mathbf{q}|$ and the "polarization vector" $|\vec{\beta}_{n\mathbf{k}}\rangle$ is defined as

$$|\vec{\beta}_{n\mathbf{k}}\rangle = \left(1+\sum_i|\tilde{p}_{i\mathbf{k}}\rangle Q_{ij}\langle\tilde{p}_{j\mathbf{k}}|\right)|\boldsymbol{\nabla}_{\mathbf{k}}\tilde{u}_{n\mathbf{k}}\rangle + i\left(\sum_{ij}|\tilde{p}_{i\mathbf{k}}\rangle Q_{ij}\langle\tilde{p}_{j\mathbf{k}}|(\mathbf{r}-\mathbf{R}_i)\right)|\tilde{u}_{n\mathbf{k}}\rangle - i\sum_{ij}|\tilde{p}_{i\mathbf{k}}\rangle\vec{\tau}_{ij}\langle\tilde{p}_{j\mathbf{k}}|\tilde{u}_{n\mathbf{k}}\rangle. \tag{30}$$

Because of the orthogonality of the one-electron states, the first term in Eq. (29) is zero, when evaluated between conduction and valence bands. Thus the final expression consists of the $\mathbf{q}$-dependent part only. The quantity $|\vec{\beta}_{n\mathbf{k}}\rangle$ [Eq. (30)] contains three components, corresponding to the three components of the nabla operator (first line), of the vectors

$(\mathbf{r}-\mathbf{R}_i)$ (second line), and the dipole term $\vec{\tau}_{ij}$. The first term is also found in the pseudopotential approximation and is simply related to the change of the cell periodic part of the wave function with respect to $\mathbf{k}$. The second one describes the change of the projector functions and the resultant change of the one-center charge with respect to $\mathbf{k}$, whereas the last term is new and compensates for the fact that the PAW wave functions are not correctly normalized, i.e., it accounts for the difference between the dipole moment of the AE and pseudo-wave-function in the PAW spheres. Formally related equations have been derived for ultrasoft pseudopotentials using Wannier functions within the Berry phase approach.[26] For conventional norm-conserving pseudopotentials $|\vec{\beta}_{n\mathbf{k}}\rangle$ reduces to the change of the wave function with respect to $\mathbf{k}$ $(\nabla_{\mathbf{k}}\tilde{u}_{n\mathbf{k}})$.

E. Derivative of the wave function with respect to k

The final quantity that needs to be determined in order to calculate $|\vec{\beta}_{n\mathbf{k}}\rangle$ is the first-order change of the wave functions with respect to $\mathbf{k}$. For this purpose we use second-order perturbation theory:

$$|\nabla_{\mathbf{k}}\tilde{u}_{n\mathbf{k}}\rangle = \sum_{n'\neq n} \frac{|\tilde{u}_{n'\mathbf{k}}\rangle\left\langle \tilde{u}_{n'\mathbf{k}}\left| \frac{\partial[\mathbf{H}(\mathbf{k})-\epsilon_{n\mathbf{k}}\mathbf{S}(\mathbf{k})]}{\partial\mathbf{k}}\right| \tilde{u}_{n\mathbf{k}}\right\rangle}{\epsilon_{n\mathbf{k}}-\epsilon_{n'\mathbf{k}}}. \tag{31}$$

Again $\mathbf{H}(\mathbf{k})$ denotes the Hamiltonian for the cell periodic wave functions, and $\mathbf{S}(\mathbf{k})$ is the corresponding overlap operator. We note that the summation over n' cannot be restricted to the conduction band states as usually done in pseudopotential methods, since the overlap operator is $\mathbf{k}$ dependent. Furthermore, the changes of the eigenenergies $\epsilon_{n\mathbf{k}}$ need to be evaluated to first order and are required to guarantee the proper orthogonalization of the first-order response. In principle, this equation is exact only for a complete set of conduction bands, but its use does not result in an additional approximation, if the calculation of the dielectric matrix is truncated at the same conduction band state as the determination of the first derivative of the wave function.

F. Static dielectric matrix using density functional perturbation theory

The previously presented set of equations exhibit the disadvantage that they require the summation over empty conduction band states. For the static dielectric function, density functional perturbation theory was suggested as an alternative approach. In this case the first order change of the wave functions ("orbital shift") with respect to $\mathbf{k}$ is determined by solving the linear Sternheimer equation[14–16,27]

$$[\mathbf{H}(\mathbf{k})-\epsilon_{n\mathbf{k}}\mathbf{S}(\mathbf{k})]|\nabla_{\mathbf{k}}\tilde{u}_{n\mathbf{k}}\rangle = -\frac{\partial[\mathbf{H}(\mathbf{k})-\epsilon_{n\mathbf{k}}\mathbf{S}(\mathbf{k})]}{\partial\mathbf{k}}|\tilde{u}_{n\mathbf{k}}\rangle \tag{32}$$

for $|\nabla_{\mathbf{k}}\tilde{u}_{n\mathbf{k}}\rangle$. Multiplication from the left by $\Sigma_{n'}|\tilde{u}_{n'\mathbf{k}}\rangle\langle\tilde{u}_{n'\mathbf{k}}|$ immediately leads to Eq. (31). The static dielectric matrix can be determined by calculating the first-order response of the wave functions $|\xi_{n\mathbf{k}}\rangle$ to an externally applied field which amounts to solving the following second linear equation[15] for $|\xi_{n\mathbf{k}}\rangle$

$$[\mathbf{H}(\mathbf{k})-\epsilon_{n\mathbf{k}}\mathbf{S}(\mathbf{k})]|\xi_{n\mathbf{k}}\rangle = -\Delta\mathbf{H}_{\mathrm{SCF}}(\mathbf{k})|\tilde{u}_{n\mathbf{k}}\rangle - |\hat{\mathbf{q}}\vec{\beta}_{n\mathbf{k}}\rangle, \tag{33}$$

where $\Delta\mathbf{H}_{\mathrm{SCF}}(\mathbf{k})$ describes the microscopic *cell periodic* change of the Hamiltonian resulting from the change of the wave functions (self-consistent field effects) to first order. In this manner, local field effects are included directly in the evaluation of the dielectric response. The previous equation has to be solved for three directions $\hat{\mathbf{q}}$ corresponding to the principal axes of the macroscopic dielectric matrix. The appropriate component of the macroscopic dielectric matrix is given by the inner-product between the first-order change of the wave function $\xi_{n\mathbf{k}}$ and the polarization vector $\vec{\beta}_{n\mathbf{k}}$:[15]

$$\varepsilon_\infty(\hat{\mathbf{q}}) = 1 - \frac{8\pi e^2}{\Omega}\sum_{v,\mathbf{k}} 2w_{\mathbf{k}}(\langle\hat{\mathbf{q}}\vec{\beta}_{v\mathbf{k}}|\xi_{v\mathbf{k}}\rangle). \tag{34}$$

The last two equations can be derived by rewriting the head of the irreducible polarizability matrix [Eq. (9)] using Eq. (29) and neglecting local field effects $[\Delta\mathbf{H}_{\mathrm{SCF}}(\mathbf{k})=0]$:

$$\chi^0_{0,0}(\mathbf{q},0) = -\frac{2|\mathbf{q}|^2}{\Omega}\sum_{c,v,\mathbf{k}} 2w_{\mathbf{k}}\frac{\langle\hat{\mathbf{q}}\vec{\beta}_{v\mathbf{k}}|\tilde{u}_{c\mathbf{k}}\rangle\langle\tilde{u}_{c\mathbf{k}}|\hat{\mathbf{q}}\vec{\beta}_{v\mathbf{k}}\rangle}{\epsilon_{c\mathbf{k}+\mathbf{q}}-\epsilon_{v\mathbf{k}}}. \tag{35}$$

Multiplication of (33) from the left with $\Sigma_{n'}|\tilde{u}_{n'\mathbf{k}}\rangle\langle\tilde{u}_{n'\mathbf{k}}|$ yields a closed equation for $|\xi_{v\mathbf{k}}\rangle$, which inserted into (34) gives the desired result, the previous equation.

III. TECHNICAL DETAILS

A. Evaluation of the macroscopic dielectric constants

The advantage of density functional perturbation theory is that all summations over empty bands have been transformed into linear equations, consequently avoiding the calculation of conduction bands. The corresponding dielectric constants will be reported as $\varepsilon^{\mathrm{LR}}_{\mathrm{mic}}$, $\varepsilon^{\mathrm{LR}}_{\mathrm{RPA}}$ and $\varepsilon^{\mathrm{LR}}_{\mathrm{DFT}}$. In the first case we neglect microscopic changes of the cell periodic potential $[\Delta H_{\mathrm{SCF}}=0$ in Eq. (33)], in the second case only changes of the Hartree potential are included in ΔH_{SCF}, whereas in the final case also changes of the exchange correlation potential are taken into account. The last value should be compared to experiment, whereas the former two are useful when comparing to literature values.

We also present results for the static dielectric constant using a summation over conduction band states without local field effects $[\varepsilon^{\mathrm{cond}}_{\mathrm{mic}}$, Eqs. (13)–(16)] and with local field effects in the RPA approximation $[\varepsilon^{\mathrm{cond}}_{\mathrm{RPA}}$, see Eq. (11)]. It is also possible to include changes of the exchange correlation potential $(\varepsilon^{\mathrm{cond}}_{\mathrm{DFT}})$ by replacing the irreducible polarizability matrix in Eq. (8) by a polarizability matrix χ^0_{xc} which includes exchange correlation effects:

TABLE I. Core radii r_c and energy cutoffs E for the PAW potentials used in the present work. Nonlocal projectors were generated for the states listed in the column "Valence." As local PAW potential a pseudopotential was generated for the states indicated in the column "Local." If the core radii for different quantum numbers are different, they are specified for each channel using a subscript.

	Valence	Local	r_c (a.u.)	E (eV)
C	$2s2p$	$3d$	$1.2_s, 1.5_p$	400
Al	$3s3p$	$3d$	1.9	240
Si	$3s3p$	$3d$	1.9	250
P	$3s3p$	$3d$	1.9	270
Ga	$4s4p4d$	$4f$	2.6	140
Ga_d	$4s4p3d4d$	$4f$	2.3	280
As	$4s4p4d$	$4f$	2.1	210

$$\chi^0_{xc} = \chi^0(1 - f_{xc}\chi^0)^{-1}. \quad (36)$$

The quantity f_{xc} is the derivative of the exchange correlation potential with respect to the charge. For details we refer to Ref. 12.

B. PAW potentials

The calculations were performed using PAW potentials in the standard local density approximation (LDA). The parameters (core radii) of the potentials and the energy cutoffs, as well as the states treated as valence states, are summarized in Table I. Two projectors are used for any of the states listed in the column "Valence." For Ga two different PAW potentials were applied, one which treats the Ga $3d$ states as core states, and a second one (Ga_d) describing the $3d$ states as valence states. For this potential one d projector was generated for the $3d$ and one for the $4d$ states. It is expected that this potential yields more precise results, in the sense that the DFT limit is obtained.

C. Brillouin zone sampling

With the exception of $\varepsilon^{\text{cond}}_{\text{RPA}}$, all static dielectric constants were determined using a $12\times12\times12$ Monkhorst-Pack grid.[28] This grid does not include the Γ point. A Monkhorst-Pack grid with $8\times8\times8$ k points yields dielectric constants within 0.02 for Si and GaAs (compare Table II), and identical values for systems with a larger gap. Except for GaAs, similar convergence can be obtained using $24\times24\times24$ k points centered at the Γ point. For GaAs, however, Γ-centered meshes converge notoriously slowly to the values obtained using Monkhorst-Pack grids as shown in Table II. This is the main reason why we have omitted such grids. The value for $\varepsilon^{\text{cond}}_{\text{RPA}}$ was determined utilizing a slightly less accurate $8\times8\times8$ Monkhorst-Pack grid, since calculations by the inversion of the full microscopic dielectric matrix are time consuming. Overall our tests indicated that even this value is converged to within 0.02, whereas convergence of other reported values is expected to be slightly better.

Convergence with respect to the conduction band states is fast for the head of the microscopic dielectric function ε_{mic}, but even if local field effects are included in the Hartree approximation, 60 conduction band states are sufficient to obtain identical values as using linear response theory (see Table II). The number of unoccupied bands was therefore set to 60 for all considered systems.

TABLE II. Ion clamped static macroscopic dielectric constants ε_∞ calculated using density functional perturbation theory and the PAW method for various k-point sets: Γ indicates a grid centered at Γ, whereas Monkhorst-Pack (MP) grids do not include the Γ point. Values for ε_{mic} neglect local field effects, whereas ε_{RPA} includes local field effects on the Hartree level. Lines starting with N_c report the dielectric constants obtained by a summation over N_c conduction band states for an $8\times8\times8$ MP grid. N_k gives the number of k points in the irreducible wedge of the Brillouin zone (IBZ) after considering the symmetry of the crystal.

GaAs	N_k (IBZ)	ε_{mic}	ε_{RPA}
$(16\times16\times16)$ Γ	145	18.16	16.55
$(24\times24\times24)$ Γ	413	15.64	14.04
$(32\times32\times32)$ Γ	897	15.14	13.56
$(48\times48\times48)$ Γ	2769	14.94	13.35
$(8\times8\times8)$ MP	60	14.76	13.30
$(12\times12\times12)$ MP	182	14.78	13.31
$N_c=10$	60	14.72	13.18
$N_c=20$	60	14.74	13.23
$N_c=40$	60	14.74	13.27
$N_c=60$	60	14.74	13.28

The dynamic dielectric function was obtained by neglecting local field effects and summing over 16 conduction band states. In this case $40\times40\times40$ k points were used and the tetrahedron method was applied for the k sampling of the Brillouin zone.

IV. RESULTS

As an example of the present approach the static macroscopic dielectric constants in various approximations are presented for the four cubic group-IV and group-III-V semiconductors (Si, SiC, AlP, and GaAs) and for cubic diamond (C). These materials crystallize in the zinc-blende and diamond structures with the lattice constants $a=5.431$, 4.350, 5.450, 5.650, and 3.567 Å, respectively. All calculations were performed at these experimental values for the lattice parameters at room temperature.

A. Static dielectric function

Table III presents the ion clamped static macroscopic dielectric constants ε_∞ calculated within the standard LDA (Ref. 29) and the PAW methodology. We will first concentrate on the "exact" results using the longitudinal expression. Obviously the results obtained by density functional perturbation theory are identical to those calculated by a summation over the conduction band states. This applies to both ε_{mic} (neglecting local fields) as well as ε_{RPA} and ε_{DFT} (including local fields in the Hartree approximation and on the

TABLE III. The ion clamped static macroscopic dielectric constants ε_∞ calculated using the PAW method and various approximations. $\varepsilon_{\mathrm{mic}}$ reports values neglecting local field effects, $\varepsilon_{\mathrm{RPA}}$ includes local field effects in the Hartree approximation, and $\varepsilon_{\mathrm{DFT}}$ includes local field effects on the DFT level. $\varepsilon^{\mathrm{cond}}$ are values obtained by summation over conduction band states, whereas $\varepsilon^{\mathrm{LR}}$ are values obtained using linear response theory (density functional perturbation theory).

Method	C	Si	SiC	AlP	GaAs	Ga_dAs
Longitudinal						
$\varepsilon_{\mathrm{mic}}^{\mathrm{LR}}$	5.98	14.08	7.29	9.12	14.77	15.18
$\varepsilon_{\mathrm{mic}}^{\mathrm{cond}}$	5.98	14.04	7.29	9.10	14.75	15.16
$\varepsilon_{\mathrm{RPA}}^{\mathrm{LR}}$	5.54	12.66	6.66	7.88	13.31	13.77
$\varepsilon_{\mathrm{RPA}}^{\mathrm{cond}}$	5.55	12.68	6.66	7.88	13.28	13.73
$\varepsilon_{\mathrm{DFT}}^{\mathrm{LR}}$	5.80	13.29	6.97	8.33	13.98	14.42
$\varepsilon_{\mathrm{DFT}}^{\mathrm{cond}}$	5.82	13.31	6.97	8.33	13.98	14.37
Transversal						
$\varepsilon_{\mathrm{mic}}^{\mathrm{cond}}$	5.68	16.50	8.00	10.63	14.72	15.33
$\varepsilon_{\mathrm{mic}}^{\mathrm{cond}}$ incl. d projectors	5.99	14.09	7.28	9.11		
$\varepsilon_{\mathrm{mic}}^{\mathrm{cond}}$ APW+LO		13.99				15.36
Experiment (Ref. 33)	5.70	11.90	6.52	7.54		11.10

DFT level, respectively). In particular, the agreement of the latter makes us confident that neglecting local field effects for the PAW one-center terms is a perfectly valid approximation: local field effects, i.e., changes of the potentials, inside the PAW spheres do not contribute to the macroscopic dielectric function.

Second, we want to comment on the transversal expression for the head of the microscopic dielectric matrix $\varepsilon_{\mathrm{mic}}^{\mathrm{cond}}$. For Si, SiC, and AlP the transversal dielectric constants are significantly larger than the longitudinal ones, whereas the results are closer for C and GaAs. A significant improvement of the agreement between transversal and longitudinal results is achieved by including d projectors and d one-center terms in the PAW spheres for Si, C, Al, and P (see Ref. 6; for GaAs the d projectors are already included, cf. Table III). As apparent from Table III, the longitudinal and transversal $\varepsilon_{\mathrm{mic}}^{\mathrm{cond}}$ now agree with typical deviations being less than 1%. We also note that the longitudinal results remain identical using the improved PAW data set with d nonlocality. This clearly shows that the transversal expression is not sufficiently accurate, if potentials are used in which the d potential is chosen as local potential, and on-site PAW terms are included only up to the p states. This is, however, the approximation widely adopted in most, if not all, PAW data sets for $2p$ and $3p$ elements.[13,17]

In the following, our results are compared to previous calculations. For Si, extensive studies were performed by Baroni and Resta.[12] For the longitudinal expression of the dielectric matrix they reported values of $\varepsilon_{\mathrm{mic}}=13.41$, $\varepsilon_{\mathrm{RPA}}=12.04$, and $\varepsilon_{\mathrm{DFT}}=12.72$. Even though our absolute values are larger by roughly 0.6, the magnitude of the local field effects are in agreement with their previous calculations. We also note that a calculation of Corso, Baroni, and Resta using density functional perturbation theory later reported a value of $\varepsilon_{\mathrm{DFT}}=12.9$ at the experimental lattice constant,[30] in better accordance with the present value of $\varepsilon_{\mathrm{DFT}}=13.3$. In passing, we note that the values are rather sensitive to the lattice constant and finite-basis-set errors. For AlP and SiC, previously reported PAW values ($\varepsilon_{\mathrm{mic}}=8.9$ and $\varepsilon_{\mathrm{mic}}=7.1$, respectively) are in agreement with the present work, whereas the value for GaAs ($\varepsilon_{\mathrm{mic}}=14.4$ in Ref. 6, when treating the $3d$ states as valence) is significantly smaller than the present one ($\varepsilon_{\mathrm{mic}}=15.3$). We found that the difference is related to the smaller LDA lattice constant and a different k-point grid used in the previous calculation. At the presently applied experimental lattice constant the gap is smaller resulting in an increase of the dielectric constant. Finally, for diamond, Brodersen *et al.*[31] obtained values of $\varepsilon_{\mathrm{mic}}=5.98$ and $\varepsilon_{\mathrm{RPA}}=5.58$, in excellent agreement with the present work.

When comparing our PAW results to all-electron FLAPW calculations published in Ref. 6, we find that the FLAPW $\varepsilon_{\mathrm{mic}}^{\mathrm{cond}}$ values for GaAs and Si are significantly smaller. To elucidate this discrepancy, we have performed calculations using the augmented plane wave plus local orbitals (APW+LO) formalism as implemented in the WIEN2K program package.[32] Compared to previous versions, the current release allows for a more accurate treatment of shallow semicore states, which is important for GaAs. As already mentioned, the convergence of the static dielectric constant with respect to Γ-centered k meshes—as usually applied in WIEN2K—turned out to be exceptionally slow for GaAs. The static dielectric constant is only sufficiently converged using a $48\times48\times48$ mesh, and the corresponding values are indicated by "APW+LO" in Table III. While the previous FLAPW $\varepsilon_{\mathrm{mic}}$ for GaAs (Si) was 12.7 (13.6),[6] the present APW+LO calculation yields $\varepsilon_{\mathrm{mic}}=15.4$ (14.0), which perfectly matches the PAW result of $\varepsilon_{\mathrm{mic}}=15.3$ (14.1) (provided that the Ga $3d$ states are properly treated). This excellent agreement supports the high accuracy of the present PAW results for both GaAs and Si. The discrepancies between the previously reported FLAPW results[6] and the current APW+LO findings for these materials can be understood in terms of three differences between these calculations: (i) the lattice parameters used, (ii) the treatment of the shallow semicore

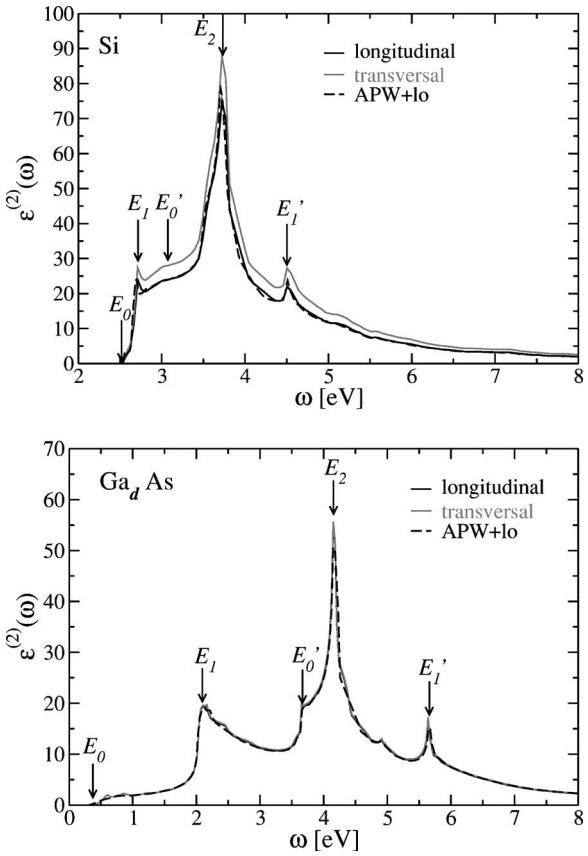

FIG. 1. The frequency-dependent imaginary part of the dielectric function obtained by the longitudinal and transversal expressions for Si and GaAs, respectively. The main optical features are indicated by arrows and labeled according to the convention introduced in Ref. 33.

states, and (iii) the improved *k*-point sampling applied in the present work.

B. Dynamic dielectric function

In Fig. 1 the frequency-dependent imaginary part of the dielectric functions is displayed for two examples Si and GaAs. For comparison, the results obtained by evaluating the longitudinal and the transversal expressions for $\varepsilon^{(2)}(\omega)$ are shown, respectively. The main optical features are indicated by arrows and labeled according to the convention introduced by Yu and Cardona.[33] For a detailed comparison, the energies of these peaks (E_0, E_1, E_2, E_0', and E_1') have been extracted from the spectra and are summarized in Table IV together with previously published PAW calculations using the transversal expression.[6] As Fig. 1 clearly demonstrates and as is also observed for the other investigated materials not shown here, the longitudinal and transversal expressions for the dynamic dielectric function yield identical results for the energy positions of these features. This is obvious, since the positions of the optical transitions are determined from the ground-state band structure (Kohn-Sham eigenvalues) by applying the optical selection rules irrespective of the type of expression for $\varepsilon_{\mathrm{mic}}(\omega)$ evaluated. Therefore, only one set of data is given in Table IV. Compared to the earlier reported

TABLE IV. The energy positions of the main optical features E_0, E_1, E_2, E_0', and E_1'. Since the peak positions are identical for the longitudinal and transversal expressions, they are stated only once. All listed values are given in units of eV.

Method	E_0	E_1	E_2	E_0'	E_1'
		Si			
PAW	2.53	2.71	3.72	3.08	4.50
APW+LO	2.54	2.70	3.71	3.08	4.51
		Ga$_d$As			
PAW	0.35	2.10	4.15	3.65	5.64
APW+LO	0.31	2.11	4.15	3.66	5.65

data,[6] the overall agreement is good. Particularly pronounced in the case of Si (and also for SiC and AlP), the peak intensities are reduced when the longitudinal expression is applied. This finding is consistent with the results discussed in the last section. Again, these differences can be compensated by the inclusion of *d* projectors and *d* one-center terms in the PAW spheres (not shown). For C and GaAs, both expressions give highly similar spectra. Since previously the discrepancies between $\varepsilon^{(2)}(\omega)$ calculated within the PAW method and the corresponding findings of the FLAPW approach could not be completely solved for GaAs,[6] we also include our APW+LO result of GaAs in Fig. 1 and Table IV. The agreement between the PAW and APW+LO dielectric functions is now extremely good, which can be understood on the grounds already emphasized above.

V. SUMMARY

The main achievement of the present work is a derivation of the head of the microscopic polarizability matrix in the longitudinal form for the PAW method. The crucial difference from the pseudopotential case is that a term describing the dipole moments inside the one-center spheres must be included. Basically, this modifies the transition probability between two states by a term which is proportional to

$$\sum_{ij} \langle \tilde{u}_{v\mathbf{k}} | \tilde{p}_{i\mathbf{k}} \rangle \tilde{\tau}_{ij} \langle \tilde{p}_{j\mathbf{k}} | \tilde{u}_{c\mathbf{k}} \rangle, \tag{37}$$

and it compensates for the fact that the PAW pseudo-wavefunctions are neither correctly normalized, nor do they possess the correct dipole moments inside the PAW spheres. The quantity τ_{ij} describes the difference of the dipole between the pseudo-partial-waves and all-electron partial waves inside the PAW spheres. A related term was derived in the context of the Berry phase approach for ultrasoft pseudopotentials using Wannier functions.[26]

In order to test the present longitudinal approach, it was applied to one insulator (C) and four semiconductors (Si, SiC, AlP, GaAs). The corresponding results were compared to the dielectric constants calculated using the simpler transversal expression. Thereby, it was shown that the convergence with respect to the number of basis functions in the PAW sphere is significantly faster for the longitudinal expression. In the case of C, Si, SiC, and AlP it turned out that

truncating the one-center expansion at $l=1$ is sufficient, whereas the transversal equation yields satisfactory results only, if the partial waves up to $l=2$ are included.

The dielectric constants were calculated in two manners. On one hand, density functional perturbation theory was applied; on the other hand, a summation over conduction band states was used. Both methods gave essentially identical results, and the convergence with respect to the number of conduction band states was also found to be rather fast. The ion clamped static dielectric constants including local field effects in the DFT approximation for C, Si, SiC, AlP, and GaAs were determined to be 5.80, 13.29, 6.97, 8.33, and 14.42. If local field effects are neglected, the respective values are 5.98, 14.08, 7.29, 9.12, and 15.18. The latter values should not be compared to experiment, but might become useful for evaluating other electronic structure methods. The reduction due to local field effects is between 3% and 9% in the investigated materials. The present values compare well with previous literature results, although they are generally slightly larger then those reported before. This applies, in particular, to Si and GaAs. To elucidate this discrepancy, full potential APW+LO calculations have been performed and we found the present PAW values confirmed to within 1%. Therefore, we believe that the present values are technically fully converged and exact within the framework of the present approximations to density functional theory. Such technically converged calculations are important, both for benchmarking electronic structure methods and as a benchmark for an improved description of the electronic correlation. The experimental values for C, Si, SiC, and AlP, and GaAs are 5.7, 11.9, 6.52, 7.54, and 11.1,[33] respectively. We therefore conclude that the present calculations clearly overestimate the dielectric constants by 5–20 %, where the overestimation is larger for small gap materials. Although this has been known for some time, the present calculations exhibit an even larger discrepancy to experiment than hereto assumed. Clearly, methods beyond the local density approximation are required for a quantitative description of screening in small gap materials.

The present work opens this possibility, i.e., it allows one to perform *GW* calculations within the framework of the PAW method. Although some calculations have already been published,[34] the Γ point has previously been avoided in the context of PAW *GW* calculations, since the required limit for small momentum transfers had not been considered. Therefore dielectric properties in the long-wavelength limit were not directly accessible using the PAW method.

ACKNOWLEDGMENTS

This work has been supported by the Austrian Fonds zur Förderung der wissenschaftlichen Forschung and by the EU Network of Excellence NANOQUANTA (Contract No. NMP4-CT-2004-500198).

*Electronic address: georg.kresse@univie.ac.at

[1] M. S. Hybertsen and S. G. Louie, Phys. Rev. B **35**, 5585 (1987).
[2] M. Städele, J. A. Majewski, P. Vogl, and A. Görling, Phys. Rev. Lett. **79**, 2089 (1997).
[3] L. J. Sham and T. M. Rice, Phys. Rev. **144**, 708 (1966).
[4] G. Strinati, Phys. Rev. B **29**, 5718 (1984).
[5] B. Adolph, V. I. Gavrilenko, K. Tenelsen, F. Bechstedt, and R. Del Sole, Phys. Rev. B **53**, 9797 (1996).
[6] B. Adolph, J. Furthmüller, and F. Bechstedt, Phys. Rev. B **63**, 125108 (2001).
[7] W. G. Schmidt, K. Seino, P. H. Hahn, F. Bechstedt, W. Lu, S. Wang, and J. Bernholc, Thin Solid Films **455–456**, 764 (2004).
[8] S. L. Adler, Phys. Rev. **126**, 413 (1962).
[9] N. Wiser, Phys. Rev. **129**, 62 (1963).
[10] M. Rohlfing and S. G. Louie, Phys. Rev. B **62**, 4927 (2000).
[11] W. G. Schmidt, S. Glutsch, P. H. Hahn, and F. Bechstedt, Phys. Rev. B **67**, 085307 (2003).
[12] S. Baroni and R. Resta, Phys. Rev. B **33**, 7017 (1986).
[13] P. E. Blöchl, Phys. Rev. B **50**, 17953 (1994).
[14] S. Baroni, P. Giannozzi, and A. Testa, Phys. Rev. Lett. **58**, 1861 (1987).
[15] P. Giannozzi, S. de Gironcoli, P. Pavone, and S. Baroni, Phys. Rev. B **43**, 7231 (1991).
[16] S. Baroni, S. de Grioncoli, A. Dal Corso, and P. Giannozzi, Rev. Mod. Phys. **73**, 515 (2001).
[17] G. Kresse and D. Joubert, Phys. Rev. B **59**, 1758 (1999).
[18] H. Ehrenreich and M. H. Cohen, Phys. Rev. **115**, 786 (1959).
[19] C. Ambrosch-Draxl and J. Sofo, cond-mat/0402523 (unpublished).
[20] A. F. Starace, Phys. Rev. A **3**, 1242 (1971).
[21] R. Del Sole and R. Girlanda, Phys. Rev. B **48**, 11789 (1993).
[22] J. Paier, R. Hirschl, M. Marsmann, and G. Kresse, J. Chem. Phys. **122**, 234102 (2005).
[23] S. H. Rhim, M. Kim, A. J. Freeman, and R. Asahi, Phys. Rev. B **71**, 045202 (2005).
[24] X. Blase, A. Rubio, S. G. Louie, and M. L. Cohen, Phys. Rev. B **52**, R2225 (1995).
[25] R. W. Godby, M. Schlüter, and L. J. Sham, Phys. Rev. B **37**, 10159 (1988).
[26] D. Vanderbilt and R. King-Smith, cond-mat/9801177 (unpublished).
[27] R. Sternheimer, Phys. Rev. **96**, 951 (1954).
[28] H. Monkhorst and J. Pack, Phys. Rev. B **13**, 5188 (1976).
[29] D. M. Ceperley and B. J. Alder, Phys. Rev. Lett. **45**, 566 (1980).
[30] A. Dal Corso, S. Baroni, and R. Resta, Phys. Rev. B **49**, 5323 (1994).
[31] S. Brodersen, D. Lukas, and W. Schattke, Phys. Rev. B **66**, 085111 (2002).
[32] P. Blaha, K. Schwarz, G. K. H. Madsen, D. Kvasnicka, and J. Luitz, Computer code WIEN2K (Vienna University of Technology, 2001), www.wien2k.at
[33] P. Y. Yu and M. Cardona, *Fundamentals of Semiconductors* (Springer-Verlag, Berlin, 2001).
[34] S. Lebégue, B. Arnaud, M. Alouani, and P. E. Blöchl, Phys. Rev. B **67**, 155208 (2003).